

# Adaptive Neural Network Stochastic-Filter-based Controller for Attitude Tracking with Disturbance Rejection

Hashim A. Hashim and Kyriakos G. Vamvoudakis

**Abstract**—This paper proposes a real-time neural network (NN) stochastic filter-based controller on the Lie Group of the Special Orthogonal Group  $SO(3)$  as a novel approach to the attitude tracking problem. The introduced solution consists of two parts: a filter and a controller. Firstly, an adaptive NN-based stochastic filter is proposed that estimates attitude components and dynamics using measurements supplied by onboard sensors directly. The filter design accounts for measurement uncertainties inherent to the attitude dynamics, namely unknown bias and noise corrupting angular velocity measurements. The closed loop signals of the proposed NN-based stochastic filter have been shown to be semi-globally uniformly ultimately bounded (SGUUB). Secondly, a novel control law on  $SO(3)$  coupled with the proposed estimator is presented. The control law addresses unknown disturbances. In addition, the closed loop signals of the proposed filter-based controller have been shown to be SGUUB. The proposed approach offers robust tracking performance by supplying the required control signal given data extracted from low-cost inertial measurement units. While the filter-based controller is presented in continuous form, the discrete implementation is also presented. Additionally, the unit-quaternion form of the proposed approach is given. The effectiveness and robustness of the proposed filter-based controller is demonstrated using its discrete form and considering low sampling rate, high initialization error, high-level of measurement uncertainties, and unknown disturbances.

**Index Terms**—Neuro-adaptive, stochastic differential equations, nonlinear filter, attitude tracking control, observer-based controller.

## I. INTRODUCTION

ATTITUDE estimation and tracking control of a rigid-body rotating in three-dimensional (3D) space are indispensable tasks for majority of robotics and aerospace applications. Examples include satellites, rotating radars, unmanned aerial vehicles (UAVs), space telescopes, to name a few [1–6]. The research in area of attitude estimation and control has made a great leap forward with the introduction of micro-electro-mechanical systems (MEMS) [7] that allowed for the design of compact low-cost onboard units such as

inertial measurement units (IMUs) and magnetic, angular rate, and gravity (MARG) sensors. Although low-cost sensors are inexpensive, low-weight, compact, and power-efficient, they supply imperfect measurements corrupted with unknown bias and noise [1,4,8]. Controlling rigid-body's rotation in 3D space requires the knowledge of the true attitude. Unfortunately, the true attitude is unknown and has to be obtained through estimation or algebraic reconstruction using, for instance IMU or MARG sensors. The algebraic attitude reconstruction involves using number of measurements and an algebraic algorithm, for instance QUEST algorithm [9] or singular value decomposition (SVD) [10]. However, algebraic reconstruction is ineffective when sensor measurements are heavily contaminated by uncertainties. As such, estimation approaches that use filtering techniques have acquired great importance [4,8,11–13].

Conventionally, attitude estimation has been addressed considering Kalman-type filters [14]. Examples include Kalman filter (KF) [11], extended Kalman filter (EKF) [8], multiplicative EKF (MEKF) [12], unscented Kalman filter (UKF) [13], and invariant EKF (IEKF) [15]. The filters in [8,11–13] are unit-quaternion based which offers nonsingularity of attitude representation, but is challenged by nonuniqueness [16]. To address the nonuniqueness limitation of unit-quaternion, a set of nonlinear attitude observing/filtering algorithms on the Special Orthogonal Group  $\mathbb{S}\mathbb{O}(3)$  have been proposed [1,4,14,17].  $\mathbb{S}\mathbb{O}(3)$  provides global and unique attitude representation [16]. Moreover, in comparison with Kalman-type filters, nonlinear attitude filtering solutions on  $\mathbb{S}\mathbb{O}(3)$  have been shown to be 1) simpler in design, 2) computationally cheap, and 3) better in terms of tracking performance [1,4,17]. With regard to attitude control, over the last two decades multiple successful control strategies have been introduced to control rigid-body's attitude given accurate attitude and angular velocity information [18–20]. Other solutions developed attitude tracking control schemes reliant on the true attitude information without angular velocity measurements [21,22]. In the above-discussed literature, attitude estimation and tracking control solutions are designed separately. However, the attitude problem is highly nonlinear and coupling a standalone filter design with a standalone controller design cannot guarantee overall stability, especially if 1) the rigid-body is equipped with a low-cost measurement unit and 2) a large initialization error is present between the true and the estimated states [2].

With an objective of overcoming the overall stability challenge, several state-of-the-art observer-based controllers have

This work was supported in part by National Sciences and Engineering Research Council of Canada (NSERC), under the grants RGPIN-2022-04937 and DGECR-2022-00103, and by NSF under grant Nos. CAREER CPS-1851588, CPS-2038589, and S&AS-1849198 and by NASA ULI under grant number 80NSSC20M0161.

\*Corresponding author, H. A. Hashim is with the Department of Mechanical and Aerospace Engineering, Carleton University, Ottawa, ON, K1S 5B6, Canada (e-mail: hhashim@carleton.ca)

K. G. Vamvoudakis is with the Daniel Guggenheim School of Aerospace Engineering, Georgia Institute of Technology, Atlanta, GA, 30332, USA e-mail: kyriakos@gatech.edu

been proposed, such as, an observer-based controller guaranteeing local exponential stability [23], a full-state observer-based controller for rigid-body motion [24], a hybrid control scheme ensuring semi-global asymptotic stability reliant on a switching observer for restoring angular velocity data [25], observer-based controller with finite time convergence [3], and observer-based controller for unknown exterior disturbances [26]. The limitations of the existing observer-based controller solutions, such as [3,23–26] are three-fold: 1) for the sake of simplicity these techniques disregard uncertainties of the onboard sensing units in the stability analysis, 2) they rely on reconstructed attitude which increases the computational cost, and 3) they only consider the case of known nonlinear dynamics of the attitude problem. However, in practice, affordable systems are likely to 1) be equipped with low-cost sensing units, 2) operate in uncertain environments where the model dynamics may not be accurately known, and 3) be affected by unknown disturbances.

Neural networks (NNs) are known to be a powerful tool for learning and estimating complex nonlinear systems [5]. Over the past few years, adaptive NNs have been shown to be efficient for online estimation of unknown high-order nonlinear dynamics. Successful applications of NNs include but are not limited to nonlinear attitude filtering [27], adaptive consensus of networked systems [28], trajectory tracking of ground robots [29], stochastic nonlinear systems [27,30], and strict-feedback multi-input multi-output systems [31]. Accurate NN estimation of unknown high-order nonlinear dynamics results in a successful control process [5,28,29]. With an objective of addressing the aforementioned shortcomings of the observer-based controllers [3,23–26], in this paper, the nonlinear attitude problem is modelled on the Lie Group of  $\mathbb{SO}(3)$  that offers global and unique attitude representation. The unknown bias and noise corrupting angular velocity measurements are tackled by incorporating stochastic differential equations in problem formulation. The measurement uncertainties, unknown disturbances, and overall stability are addressed through proposing NN stochastic filter-based controller for the attitude tracking problem. The contributions of this paper are as follows:

- 1) A real-time NN-based nonlinear stochastic filter able to use available measurements directly for the attitude estimation problem is proposed on  $\mathbb{SO}(3)$ ;
- 2) The proposed NN-based filter considers unknown random noise as well as constant bias corrupting the velocity measurement;
- 3) Using Lyapunov stability, the closed loop error signals of the stochastic filter design are guaranteed to be semi-globally uniformly ultimately bounded (SGUUB) in mean square;
- 4) A control law has been proposed considering states estimated by the NN-based filter, uncertain measurements, and unknown disturbances;
- 5) The overall stability has been proven, and the closed loop error signals of the filter-based controller have been shown to be SGUUB using Lyapunov stability;

To the best of our knowledge, the attitude tracking problem

has not been previously addressed using NN-based nonlinear stochastic filter-based controller on  $\mathbb{SO}(3)$ . The proposed approach is robust against disturbances and can be a perfect fit for systems equipped with low-cost sensing units. Furthermore, the proposed approach provides strong tracking performance, is computationally cheap, and has been tested in its discrete form at a low sampling rate.

The paper is organized to contain eight Sections. Section II introduces preliminaries and math notation related to attitude and  $\mathbb{SO}(3)$ . Section III outlines the attitude problem, presents the sensor measurements, error criteria, and formulates the problem with respect to stochastic differential equations. Section IV presents NN approximation of the nonlinear attitude problem and proposes a novel NN-based stochastic attitude filter. Section V introduces the control law and the innovation terms. Section VI presents a summary of the implementation in a discrete form. Section VII demonstrates the numerical results. Section VIII concludes the work.

## II. PRELIMINARIES

$\mathbb{R}$  and  $\mathbb{R}_+$  refer to a set of real numbers and nonnegative real numbers, respectively, while  $\mathbb{R}^{n \times m}$  stands for an  $n$ -by- $m$  dimensional space.  $\mathbf{I}_n \in \mathbb{R}^{n \times n}$  describes an identity matrix, and  $0_{n \times m} \in \mathbb{R}^{n \times m}$  represents a matrix of zeros.  $\|u\| = \sqrt{u^\top u}$  denotes the Euclidean norm of  $u \in \mathbb{R}^n$ .  $\|W\|_F = \sqrt{\text{Tr}\{WW^*\}}$  refers to the Frobenius norm of matrix  $W \in \mathbb{R}^{q \times m}$  with  $*$  standing for a conjugate transpose.  $\exp(\cdot)$ ,  $\mathbb{P}\{\cdot\}$ , and  $\mathbb{E}[\cdot]$  refers to an exponential, a probability, and an expected value of a component. Let us define  $A \in \mathbb{R}^{n \times n}$  with  $\lambda(A) = \{\lambda_1, \lambda_2, \dots, \lambda_n\}$  being a set of eigenvalues.  $\bar{\lambda}_A = \bar{\lambda}(A)$  represents the maximum value, and  $\underline{\lambda}_A = \underline{\lambda}(A)$  stands for the minimum value of  $\lambda(A)$ . For simplicity,  $\{\mathcal{I}\}$  denotes a fixed inertial-frame and  $\{\mathcal{B}\}$  stands for a fixed body-frame. Orientation of a rigid-body is known as attitude  $R \in \mathbb{SO}(3)$  described by

$$\mathbb{SO}(3) = \{R \in \mathbb{R}^{3 \times 3} | R^\top R = \mathbf{I}_3, \det(R) = +1\}$$

with  $\det(\cdot)$  denoting a determinant.  $\mathfrak{so}(3)$  describes the Lie algebra of  $\mathbb{SO}(3)$  given by

$$\mathfrak{so}(3) = \{[u]_\times \in \mathbb{R}^{3 \times 3} | [u]_\times^\top = -[u]_\times, u \in \mathbb{R}^3\}$$

$$[u]_\times = \begin{bmatrix} 0 & -u_3 & u_2 \\ u_3 & 0 & -u_1 \\ -u_2 & u_1 & 0 \end{bmatrix} \in \mathfrak{so}(3), \quad u = \begin{bmatrix} u_1 \\ u_2 \\ u_3 \end{bmatrix}$$

$\mathbf{vex}$  defines the inverse mapping of  $[\cdot]_\times$  where  $\mathbf{vex} : \mathfrak{so}(3) \rightarrow \mathbb{R}^3$  such that  $\mathbf{vex}([u]_\times) = u, \forall u \in \mathbb{R}^3$  while  $\mathcal{P}_a : \mathbb{R}^{3 \times 3} \rightarrow \mathfrak{so}(3)$  is an anti-symmetric projection operator where

$$\mathcal{P}_a(A) = \frac{1}{2}(A - A^\top) \in \mathfrak{so}(3), \forall A \in \mathbb{R}^{3 \times 3}$$

Consider  $A = [a_{i,j}]_{i,j=1,2,3} \in \mathbb{R}^{3 \times 3}$  and define

$$\Upsilon(A) = \mathbf{vex}(\mathcal{P}_a(A)) = \frac{1}{2} \begin{bmatrix} a_{32} - a_{23} \\ a_{13} - a_{31} \\ a_{21} - a_{12} \end{bmatrix} \in \mathbb{R}^3 \quad (1)$$

Define the Euclidean distance of  $R$

$$\|R\|_1 = \frac{1}{4} \text{Tr}\{\mathbf{I}_3 - R\} \in [0, 1], \quad R \in \mathbb{SO}(3) \quad (2)$$

with  $\text{Tr}\{\cdot\}$  referring to a trace of a matrix (visit [4,14]). Let  $R \in \text{SO}(3)$ ,  $Z \in \mathbb{R}^{3 \times 3}$ ,  $y, z \in \mathbb{R}^3$  and recall the composition mapping in (1). The identities below hold true and will be useful in the subsequent derivations:

$$z \times y = yz^\top - zy^\top \quad (3)$$

$$R[y]_\times R^\top = [Ry]_\times \quad (4)$$

$$\text{Tr}\{Z[y]_\times\} = \text{Tr}\{\mathcal{P}_a(Z)[y]_\times\} = -2\Upsilon(Z)^\top y \quad (5)$$

### III. PROBLEM FORMULATION

#### A. Attitude Dynamics and Measurements

Consider  $R \in \text{SO}(3)$  as the rigid-body's attitude and  $\Omega$  as the rigid-body's angular velocity where  $R, \Omega \in \{\mathcal{B}\}$ . The true attitude and angular velocity dynamics are given by

$$\begin{cases} \dot{R} &= R[\Omega]_\times \\ J\dot{\Omega} &= [J\Omega]_\times \Omega + \mathcal{T} + d \end{cases} \quad (6)$$

where  $J = J^\top \in \mathbb{R}^{3 \times 3}$  denotes the rigid-body's inertia matrix (positive-definite),  $\mathcal{T} \in \mathbb{R}^3$  stands for the rotational torque (control input signal), and  $d \in \mathbb{R}^3$  denotes an unknown constant disturbance vector with  $J, \mathcal{T}, d \in \{\mathcal{B}\}$ . The attitude can be defined using a set of  $N$  observations in  $\{\mathcal{I}\}$  and  $N$  respective measurements in  $\{\mathcal{B}\}$ . Note that, at least two non-collinear observations and measurements must be available. Examples of common low-cost units for attitude determination and estimation include [1,4,11,14,32]:

- An inertial measurement unit (IMU) composed of a gyroscope (supplies angular velocity measurements), a magnetometer (supplies direction of the Earth's magnetic field), and an accelerometer (supplies apparent acceleration measurements) or
- A magnetic, angular rate, and gravity (MARG) sensor.

Define  $r_i \in \mathbb{R}^3$  as the  $i$ th observation in  $\{\mathcal{I}\}$  and  $y_i \in \mathbb{R}^3$  as the  $i$ th measurement in  $\{\mathcal{B}\}$  for all  $i = 1, 2, \dots, N$ . The  $i$ th measurement  $y_i$  is defined by [4,14,32,33]

$$y_i = R^\top r_i + b_i + n_i \in \mathbb{R}^3, \quad \forall i = 1, 2, \dots, N \quad (7)$$

where  $b_i$  is unknown constant bias and  $n_i$  refers to unknown noise. The expression in (7) exemplifies measurements supplied by an IMU such as a magnetometer and an accelerometer. It is a common approach to normalize inertial-frame observations and body-frame measurements as follows:

$$\mathbf{r}_i = \frac{r_i}{\|r_i\|}, \quad \mathbf{y}_i = \frac{y_i}{\|y_i\|} \quad (8)$$

An angular velocity measurement is given by:

$$\Omega_m = \Omega + W_b + n \in \mathbb{R}^3 \quad (9)$$

where  $\Omega$  refers to the true angular velocity, while  $W_b$  and  $n$  describe unknown weighted bias (constant) and noise.

#### B. Stochastic Reformulation

In (9)  $n$  is a bounded Gaussian noise vector with  $\mathbb{E}[n] = 0$ . Considering the fact that a derivative of a Gaussian process leads to a Gaussian process [4,34,35], one can re-express the noise vector  $n$  in terms of Brownian motion process as follows:

$$n = \mathcal{Q} \frac{d\beta}{dt} \quad (10)$$

where  $\beta \in \mathbb{R}^3$ , and  $\mathcal{Q} = \mathcal{Q}^\top \in \mathbb{R}^{3 \times 3}$  refers to an unknown weighted matrix with  $\mathcal{Q}^2 = \mathcal{Q}\mathcal{Q}^\top$  being the noise covariance. Note that  $\mathbb{P}\{\beta(0) = 0\} = 1$  and  $\mathbb{E}[\beta] = 0$  [34]. Hence, from (9) and (10), the upper portion of the true attitude dynamics in (6) are re-expressed in a stochastic form as below:

$$dR = R[\Omega_m - W_b]_\times dt - R[\mathcal{Q}d\beta]_\times \quad (11)$$

According to (1)-(5), it becomes apparent that the Euclidean distance of the attitude stochastic dynamics in (11) is equivalent to

$$d\|R\|_{\text{I}} = \frac{1}{2} \Upsilon(R)^\top (\Omega_m - b) dt - \frac{1}{2} \Upsilon(R)^\top \mathcal{Q} d\beta \quad (12)$$

**Definition 1.** [4,36] Consider the dynamics in (12) and let  $t_{in}$  be an initial time.  $\|R\|_{\text{I}} = \|R(t)\|_{\text{I}}$  is defined to be almost SGUUB if for a known set  $S_\rho \in \mathbb{R}$  and  $\|R(t_{in})\|_{\text{I}}$  there exists a constant  $c > 0$  and a time constant  $\tau_c = \tau_c(\eta, \|R(t_{in})\|_{\text{I}})$  with  $\mathbb{E}[\|R(t_{in})\|_{\text{I}}] < c, \forall t > t_{in} + c$ .

**Lemma 1.** [37] Consider the dynamics in (12) and let  $\mathcal{U}(\|R\|_{\text{I}})$  be a twice differentiable cost function with the following differential operator:

$$\mathcal{L}\mathcal{U}(\|R\|_{\text{I}}) = \mathcal{U}_1^\top f + \frac{1}{2} \text{Tr}\{gg^\top \mathcal{U}_2\} \quad (13)$$

where  $f = \frac{1}{2} \Upsilon(R)^\top (\Omega_m - W_b) \in \mathbb{R}$ ,  $g = -\frac{1}{2} \Upsilon(R)^\top \mathcal{Q} \in \mathbb{R}^{1 \times 3}$ ,  $\mathcal{U}_1 = \partial \mathcal{U} / \partial \|R\|_{\text{I}}$ , and  $\mathcal{U}_2 = \partial^2 \mathcal{U} / \partial \|R\|_{\text{I}}^2$ . Define  $\underline{\rho}_1(\cdot)$  and  $\bar{\rho}_2(\cdot)$  as class  $\mathcal{K}_\infty$  functions, and let  $\mu_1 > 0$  and  $\mu_2 \geq 0$  where

$$\underline{\rho}_1(\|R\|_{\text{I}}) \leq \mathcal{U}(\|R\|_{\text{I}}) \leq \bar{\rho}_2(\|R\|_{\text{I}}) \quad (14)$$

$$\begin{aligned} \mathcal{L}\mathcal{U}(\|R\|_{\text{I}}) &= \mathcal{U}_1^\top f + \frac{1}{2} \text{Tr}\{gg^\top \mathcal{U}_2\} \\ &\leq -\mu_1 \mathcal{U}(\|R\|_{\text{I}}) + \mu_2 \end{aligned} \quad (15)$$

Thereby, the dynamics in (12) have an almost unique strong solution on  $[0, \infty)$ . Additionally, the solution  $\|R\|_{\text{I}}$  is bounded in probability by

$$\mathbb{E}[\mathcal{U}(\|R\|_{\text{I}})] \leq \mathcal{U}(\|R(0)\|_{\text{I}}) \exp(-\mu_1 t) + \mu_2 / \mu_1 \quad (16)$$

Moreover, the expression in (16) indicates that  $\|R\|_{\text{I}}$  is SGUUB.

**Lemma 2.** [4] Let  $R \in \text{SO}(3)$ ,  $M = M^\top \in \mathbb{R}^{3 \times 3}$  with  $\text{rank}(M) \geq 2$ , and  $\bar{M} = \text{Tr}\{M\} \mathbf{I}_3 - M$ . Then, the following definitions hold:

$$\underline{\lambda}_{\bar{M}}^2 \|R\|_{\text{I}} \leq \|\Upsilon(MR)\|^2 \leq \bar{\lambda}_{\bar{M}}^2 \|R\|_{\text{I}} \quad (17)$$

This work aims to develop a real-time NN stochastic filter-based controller for the attitude tracking problem of a rigid-body in 3D space. An adaptive NN-based stochastic filter on  $SO(3)$  will be proposed for estimating the attitude

components, dynamics, and angular velocity uncertainties (unknown constant covariance and bias) using onboard sensor measurements directly. NN weights will be updated online and the adaptation mechanism will be extracted using a novel Lyapunov function candidate. Next, a control law on  $SO(3)$  interconnected with the proposed filter will be presented. The control law will account for unknown disturbances affecting the rigid-body. Fig. 1 presents a conceptual summary of the proposed methodology.

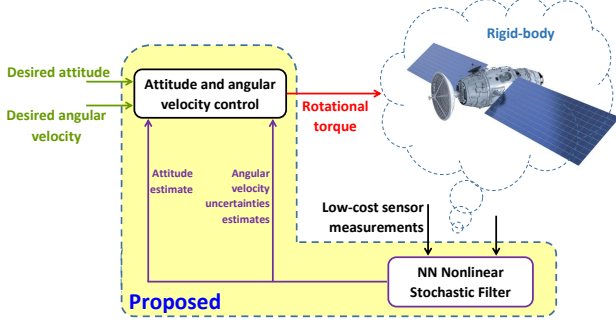


Fig. 1. Illustrative diagram of the proposed filter-based controller for the attitude tracking problem.

#### IV. NEURAL NETWORK-BASED STOCHASTIC FILTER

In this Section, our goal is to design a real-time NN-based nonlinear stochastic filter for the attitude estimation problem that uses available measurements directly without attitude reconstruction. Let us define  $\hat{R} \in \mathbb{S}\mathbb{O}(3)$  as the estimate of  $R$ . Let the estimation error be defined as

$$\tilde{R}_o = R^\top \hat{R} \in \mathbb{S}\mathbb{O}(3) \quad (18)$$

Let us define  $\hat{W}_b$  as the estimate of  $W_b$  in (9). Define the filter dynamics as follows:

$$\dot{\hat{R}} = \hat{R}[\Omega_m - \hat{W}_b - C]_\times \quad (19)$$

where  $C \in \mathbb{R}^3$  refers to a correction matrix,  $\hat{W}_b \in \mathbb{R}^{3 \times 1}$  being the estimate of  $W_b$  in (9), and  $C$  and  $\hat{W}_b$  will be designed subsequently. Let the estimation error between  $W_b$  and  $\hat{W}_b$  be as follows:

$$\tilde{W}_b = W_b - \hat{W}_b \in \mathbb{R}^3 \quad (20)$$

##### A. Direct Measurement Setup

In view of the vector measurements in (7), let us introduce the following variable:

$$\hat{y}_i = \hat{R}^\top \mathbf{r}_i \quad (21)$$

From (8), define the following two variables

$$\begin{cases} M_r &= \sum_{i=1}^N s_i \mathbf{r}_i \mathbf{r}_i^\top \\ M_y &= \sum_{i=1}^N s_i \mathbf{y}_i \mathbf{y}_i^\top = \sum_{i=1}^N s_i R^\top \mathbf{r}_i \mathbf{r}_i^\top R = R^\top M_r R \end{cases} \quad (22)$$

where  $s_i$  denotes confidence measure of the  $i$ th observation/measurement. For the stability analysis, let us redefine the expression in (7) as  $\mathbf{y}_i = R^\top \mathbf{r}_i$ . Consequently, one finds

$$M_y \tilde{R}_o = \sum_{i=1}^N s_i \mathbf{y}_i \mathbf{y}_i^\top R^\top \hat{R} = \sum_{i=1}^N s_i \mathbf{y}_i \hat{y}_i^\top \quad (23)$$

From (1) and (23), one shows

$$\begin{aligned} \Upsilon(M_y \tilde{R}_o) &= \frac{1}{2} \mathbf{vex}(M_y \tilde{R}_o - \tilde{R}_o^\top M_y^\top) \\ &= \frac{1}{2} \mathbf{vex}\left(\sum_{i=1}^N s_i \mathbf{y}_i \hat{y}_i^\top - \sum_{i=1}^N s_i \hat{y}_i \mathbf{y}_i^\top\right) \\ &= \sum_{i=1}^n \frac{s_i}{2} \hat{y}_i \times \mathbf{y}_i \end{aligned} \quad (24)$$

Likewise, for  $\|M_y \tilde{R}_o\|_I = \frac{1}{4} \text{Tr}\{M_y - M_y \tilde{R}_o\}$  and in view of (23), one obtains

$$\begin{aligned} \|M_y \tilde{R}_o\|_I &= \frac{1}{4} \text{Tr}\left\{\sum_{i=1}^N s_i \mathbf{y}_i \mathbf{y}_i^\top - \sum_{i=1}^N s_i \mathbf{y}_i \hat{y}_i^\top\right\} \\ &= \frac{1}{4} \text{Tr}\left\{\sum_{i=1}^N s_i \mathbf{y}_i (\mathbf{y}_i - \hat{y}_i)^\top\right\} \end{aligned} \quad (25)$$

##### B. Error Dynamics and NN Approximation

From (6), (20), and (31), the error dynamics are as follows:

$$\begin{aligned} d\tilde{R}_o &= R^\top d\hat{R} + dR^\top \hat{R} \\ &= (\tilde{R}_o[\Omega + \tilde{W}_b - C]_\times + [\Omega]_\times^\top \tilde{R}_o)dt + \tilde{R}_o[Qd\beta]_\times \\ &= \tilde{R}_o[\Omega]_\times - [\Omega]_\times \tilde{R}_o + \tilde{R}_o[\tilde{W}_b - C]_\times dt + \tilde{R}_o[Qd\beta]_\times \end{aligned} \quad (26)$$

One can show that

$$\begin{aligned} \dot{M}_y &= R^\top M_r R[\Omega]_\times - [\Omega]_\times R^\top M_r R \\ &= M_y[\Omega]_\times - [\Omega]_\times M_y \end{aligned}$$

Let us define  $\|M_y \tilde{R}_o\|_I = \frac{1}{4} \text{Tr}\{M_y(\mathbf{I}_3 - \tilde{R}_o)\}$ . Based on (5) and (26), one finds that the Euclidean distance of (26) is as follows:

$$\begin{aligned} d\|M_y \tilde{R}_o\|_I &= -\frac{1}{4} \text{Tr}\{M_y d\tilde{R}_o\} \\ &= -\frac{1}{4} \text{Tr}\{M_y \tilde{R}_o[(\tilde{W}_b - C)dt + Qd\beta]_\times\} \end{aligned} \quad (27)$$

with  $\text{Tr}\{\dot{M}_y\} = \text{Tr}\{M_y[\Omega]_\times - [\Omega]_\times M_y\} = 0$  and  $\text{Tr}\{M_y \tilde{R}_o[\Omega]_\times - [\Omega]_\times M_y \tilde{R}_o\} = 0$ . In this work, linear in parameter structure of NNs is adopted. For  $x \in \mathbb{R}^n$  and a function  $f = f(x) \in \mathbb{R}^m$ , the linear NN weights structure is approximated as follows:

$$f = W^\top \varphi(x) + \alpha_f \quad (28)$$

with  $W \in \mathbb{R}^{q \times m}$  being a matrix of synaptic weights,  $\varphi(x) \in \mathbb{R}^q$  standing for an activation function, and  $\alpha_f \in \mathbb{R}^m$  describing an approximated error vector. The activation function can have high-order connection elements, for example, Gaussian functions, radial basis functions (RBFs) [38], and sigmoid functions [27,39]. Our strategy is to reach accurate

attitude and gyro bias estimation as well as attenuate gyro noise *stochasticity* effect which, in turn, will result in accurate estimation of nonlinear attitude dynamics. NNs have the potential of successfully estimating high-order nonlinear dynamics [5,28,29]. Define  $\varphi(\mathbf{Y}_o) = \varphi(\mathbf{Y}(M_y \tilde{R}_o)) \in \mathbb{R}^{q \times 1}$  as an activation function, and consider approximating

$$\begin{aligned} \mathbf{Y}_o(\tilde{W}_b - C) &= (\tilde{W}_b - C)\Gamma_b^\top \varphi(\mathbf{Y}_o)^\top + \alpha_b \\ \mathcal{Q}\mathbf{Y}_o &= W_\sigma^\top \varphi(\mathbf{Y}_o) + \alpha_\sigma \end{aligned}$$

with  $q$  being a positive integer that stands for the number of neurons,  $\Gamma_b \in \mathbb{R}^{q \times 3}$  referring to a constant matrix,  $W_\sigma \in \mathbb{R}^{q \times 3}$  denoting unknown NN weighed matrix to be later adaptively estimated and tuned,  $C \in \mathbb{R}^{3 \times 1}$  being an innovation (correction) term, and  $\alpha_b \in \mathbb{R}$  and  $\alpha_\sigma \in \mathbb{R}^3$  being the approximated errors. It is worth noting that  $\alpha_b \rightarrow 0$  and  $\|\alpha_\sigma\| \rightarrow 0$  as  $q \rightarrow \infty$ . In view of the nonlinear dynamics in (27) and the expression in (28), one obtains

$$\begin{aligned} d\|M_y \tilde{R}_o\|_I &= \underbrace{\frac{1}{2}(\varphi(\mathbf{Y}_o)^\top \Gamma_b (\tilde{W}_b - C) + \alpha_b)}_f dt \\ &+ \underbrace{\frac{1}{2}(\varphi(\mathbf{Y}_o)^\top W_\sigma + \alpha_\sigma^\top)}_g d\beta \end{aligned} \quad (29)$$

with  $\varphi(\mathbf{Y}_o) = \varphi(\mathbf{Y}(M_y \tilde{R}_o)) \in \mathbb{R}^{q \times 1}$  being an activation function, and  $\alpha_b \in \mathbb{R}$  and  $\alpha_\sigma \in \mathbb{R}^3$ . Define  $\bar{W}_\sigma = W_\sigma W_\sigma^\top$  where  $\hat{W}_\sigma$  is the estimate of  $\bar{W}_\sigma$ . Let the estimation error between  $\bar{W}_\sigma$  and  $\hat{W}_\sigma$  be defined as follows:

$$\tilde{W}_\sigma = \bar{W}_\sigma - \hat{W}_\sigma \in \mathbb{R}^{q \times q} \quad (30)$$

### C. Direct NN-based Stochastic Filter

Consider the following direct real-time NN-based stochastic filter design:

$$\begin{cases} \dot{\hat{R}} &= \hat{R}[\Omega_m - \hat{W}_b - C] \times \\ C &= \left( \Gamma_b^\top \mathbf{I}_3 + \frac{\Psi_2}{4\Psi_1} (\Gamma_b^\top \Gamma_b)^{-1} \Gamma_b^\top \hat{W}_\sigma \right) \varphi(\mathbf{Y}_o) \\ \dot{\hat{W}}_b &= \gamma_b (\Psi_1 \Gamma_b \varphi(\mathbf{Y}_o) - k_{ob} \hat{W}_b) \\ \dot{\hat{W}}_\sigma &= \frac{\Psi_2}{4} \Gamma_\sigma \varphi(\mathbf{Y}_o) \varphi(\mathbf{Y}_o)^\top - k_{o\sigma} \Gamma_\sigma \hat{W}_\sigma \end{cases} \quad (31)$$

where

$$\begin{cases} \|M_y \tilde{R}_o\|_I &= \frac{1}{4} \text{Tr} \{ \sum_{i=1}^N s_i \mathbf{y}_i (\mathbf{y}_i - \hat{\mathbf{y}}_i)^\top \} \\ \mathbf{Y}_o &= \mathbf{Y}(M_y \tilde{R}_o) = \sum_{i=1}^N \frac{s_i}{2} \hat{\mathbf{y}}_i \times \mathbf{y}_i \\ \Psi_1 &= (\|M_y \tilde{R}_o\|_I + 1) \exp(\|M_y \tilde{R}_o\|_I) \\ \Psi_2 &= (\|M_y \tilde{R}_o\|_I + 2) \exp(\|M_y \tilde{R}_o\|_I) \end{cases} \quad (32)$$

with  $k_{ob}, k_{o\sigma}, \gamma_b \in \mathbb{R}$  being positive constants,  $\Gamma_\sigma \in \mathbb{R}^{q \times q}$  being a positive diagonal matrix,  $\Gamma_b \in \mathbb{R}^{q \times 3}$  which is selected such that  $\Gamma_b^\top \Gamma_b$  is positive definite,  $q$  denoting neurons number, and  $\hat{W}_b \in \mathbb{R}^{3 \times 3}$  and  $\hat{W}_\sigma \in \mathbb{R}^{q \times q}$  being the estimated weights of  $W_b$  and  $W_\sigma$ , respectively.  $\varphi(\mathbf{Y}_o)$  denotes an activation function. It is obvious that  $\hat{W}_\sigma$  is symmetric provided that  $\hat{W}_\sigma(0) = \hat{W}_\sigma(0)^\top$ .

**Theorem 1.** Consider the stochastic system in (11). Assume that at least two observations and their respective measurements in (7) are available. Couple the NN-based stochastic

filter in (31) directly with the measurements in (9) ( $\Omega_m = \Omega + W_b + n$ ) and (7) ( $y_i = R^\top r_i \forall i = 1, 2, \dots, N$ ). Let  $\|\tilde{R}_o(0)\|_I \neq +1$  (unstable equilibria). Thus, the closed-loop error signals ( $\|\tilde{R}_o\|_I, \tilde{W}_b, \tilde{W}_\sigma$ ) are SGUUB in the mean square.

*Proof:* Define a Lyapunov function candidate  $\mathcal{U}_o = \mathcal{U}_o(\|M_y \tilde{R}_o\|_I, \tilde{W}_b, \tilde{W}_\sigma)$  such that

$$\begin{aligned} \mathcal{U}_o &= \frac{1}{2} \exp(\|M_y \tilde{R}_o\|_I) \|M_y \tilde{R}_o\|_I + \frac{1}{2\gamma_b} \tilde{W}_b^\top \tilde{W}_b \\ &+ \frac{1}{2} \text{Tr} \{ \tilde{W}_\sigma^\top \Gamma_\sigma^{-1} \tilde{W}_\sigma \} \end{aligned} \quad (33)$$

where  $\mathcal{U}_o : \text{SO}(3) \times \mathbb{R}^3 \times \mathbb{R}^{q \times q} \rightarrow \mathbb{R}_+$ . Define  $\bar{M}_y = \text{Tr}\{M_y\} \mathbf{I}_3 - M_y$  and recall Lemma 2. Since  $1 \leq \exp(\|\tilde{R}_o\|_I) < 3$  [40], let us define  $\underline{\delta} = \inf_{t \geq 0} \frac{\lambda \bar{M}}{4}$  where  $\inf$  denotes the infimum and  $\bar{\delta} = \sup_{t \geq 0} \exp(\frac{\lambda \bar{M}}{2})$  with  $\sup$  representing the supremum. Hence, one obtains

$$e_o^\top H_1 e_o \leq \mathcal{U}_o \leq e_o^\top H_2 e_o$$

where

$$\lambda(H_1) \|e_o\|^2 \leq \mathcal{U}_o \leq \bar{\lambda}(H_2) \|e_o\|^2$$

with  $H_1 = \text{diag}(\delta^2, \frac{\gamma_b}{2}, \frac{1}{2} \lambda(\Gamma_\sigma^{-1}))$ ,  $H_2 = \text{diag}(3\bar{\delta}^2, \frac{\gamma_b}{2}, \frac{1}{2} \bar{\lambda}(\Gamma_\sigma^{-1}))$ , and  $e_o = [\sqrt{\|\tilde{R}_o\|_I}, \|\tilde{W}_b\|, \|\tilde{W}_\sigma\|_F]^\top$ . Owing to the fact that  $\delta, \bar{\delta}, \gamma_b, \lambda(\Gamma_\sigma^{-1}), \bar{\lambda}(\Gamma_\sigma^{-1}) > 0$ , it becomes apparent that  $\lambda(H_1) > 0$  and  $\bar{\lambda}(H_2) > 0$  which indicates that  $\mathcal{U}_o > 0$  for all  $e_o \in \mathbb{R}^3 \setminus \{0\}$ . One is able to show that the first  $\frac{\partial \mathcal{U}_o}{\partial \|M_y \tilde{R}_o\|_I} = \frac{\Psi_1}{2}$  and second  $\frac{\partial^2 \mathcal{U}_o}{\partial \|M_y \tilde{R}_o\|_I^2} = \frac{\Psi_2}{2}$  partial derivatives of  $\mathcal{U}_o$  relative to  $\|M_y \tilde{R}_o\|_I$  are as follows:

$$\begin{cases} \Psi_1 &= (1 + \|M_y \tilde{R}_o\|_I) \exp(\|M_y \tilde{R}_o\|_I) \\ \Psi_2 &= (2 + \|M_y \tilde{R}_o\|_I) \exp(\|M_y \tilde{R}_o\|_I) \end{cases} \quad (34)$$

Therefore, in view of (29), (33), (34), and Lemma 1, one obtains the following differential operator:

$$\begin{aligned} \mathcal{L}\mathcal{U}_o &= \Psi_1 f + \frac{1}{2} \text{Tr} \{ g g^\top \Psi_2 \} - \frac{1}{\gamma_b} \tilde{W}_b^\top \dot{\tilde{W}}_b \\ &- \text{Tr} \{ \tilde{W}_\sigma^\top \Gamma_\sigma^{-1} \dot{\tilde{W}}_\sigma \} \end{aligned} \quad (35)$$

From (31) and (35), one finds

$$\begin{aligned} \mathcal{L}\mathcal{U}_o &= \Psi_1 (\varphi(\mathbf{Y}_o)^\top \Gamma_b (\tilde{W}_b - C) + \alpha_b) \\ &+ \frac{\Psi_2}{8} \text{Tr} \{ (W_\sigma^\top \varphi(\mathbf{Y}_o) + \alpha_\sigma) (W_\sigma^\top \varphi(\mathbf{Y}_o) + \alpha_\sigma)^\top \} \\ &- \frac{1}{\gamma_b} \tilde{W}_b^\top \dot{\tilde{W}}_b - \text{Tr} \{ \tilde{W}_\sigma^\top \Gamma_\sigma^{-1} \dot{\tilde{W}}_\sigma \} \\ &\leq \Psi_1 \varphi(\mathbf{Y}_o)^\top \Gamma_b (\tilde{W}_b - C) \\ &+ \frac{\Psi_2}{4} \text{Tr} \{ \bar{W}_\sigma \varphi(\mathbf{Y}_o) \varphi(\mathbf{Y}_o)^\top \} - \frac{1}{\gamma_b} \tilde{W}_b^\top \dot{\tilde{W}}_b \\ &- \text{Tr} \{ \tilde{W}_\sigma^\top \Gamma_\sigma^{-1} \dot{\tilde{W}}_\sigma \} + \Psi_1 \alpha_b + \frac{\Psi_2}{4} \|\alpha_\sigma\|^2 \end{aligned} \quad (36)$$

where *Young's inequality* has been applied to the following expression:  $\alpha_\sigma^\top W_\sigma^\top \varphi(\mathbf{Y}_o) = \frac{1}{2} \varphi(\mathbf{Y}_o)^\top \bar{W}_\sigma \varphi(\mathbf{Y}_o) + \frac{1}{2} \|\alpha_\sigma\|^2$ . Let us define  $\epsilon_1 = \sup_{t \geq 0} \Psi_1$  and  $\epsilon_2 = \sup_{t \geq 0} \Psi_2$ . From (20) and (30), substitute  $\bar{W}_\sigma$  in (31) for  $\bar{W}_\sigma = \hat{W}_\sigma + \tilde{W}_\sigma$ . Thereby,

utilizing  $\dot{\tilde{W}}_b$ ,  $\dot{\tilde{W}}_\sigma$ , and  $C$  definitions in (31), the result in (36) can be rewritten as follows:

$$\begin{aligned} \mathcal{L}\mathcal{U}_o &\leq -\|\Gamma_b^\top \varphi(\mathbf{Y}_o)\|^2 - k_{bo}\|\tilde{W}_b\|^2 + k_{bo}\|\tilde{W}_b\|\|\tilde{W}_b\| \\ &\quad - k_{\sigma o}\|\tilde{W}_\sigma\|_F^2 + k_{\sigma o}\|\tilde{W}_\sigma\|_F\|\tilde{W}_\sigma\|_F + \epsilon_1\alpha_b \\ &\quad + \frac{\epsilon_2}{4}\|\alpha_\sigma\|^2 \end{aligned} \quad (37)$$

On the basis of *Young's inequality*  $\|\tilde{W}_b\|\|\tilde{W}_b\| \leq \frac{1}{2}\|\tilde{W}_b\|^2 + \frac{1}{2}\|\tilde{W}_b\|^2$  and  $\|\tilde{W}_\sigma\|_F\|\tilde{W}_\sigma\|_F \leq \frac{1}{2}\|\tilde{W}_\sigma\|_F^2 + \|\tilde{W}_\sigma\|_F^2$ . Let us select a hyperbolic tangent activation function  $\varphi(\alpha) = \frac{\exp(\alpha) - \exp(-\alpha)}{\exp(\alpha) + \exp(-\alpha)}$  with  $\alpha \in \mathbb{R}$ . It becomes apparent that  $4\|\Gamma_b^\top \varphi(\mathbf{Y}(\tilde{R}))\|^2 \geq k_{co}\|\mathbf{Y}(\tilde{R})\|^2$  where  $k_{co} = \lambda(\Gamma_b^\top \Gamma_b)$ . As such, one finds

$$\mathcal{L}\mathcal{U}_o \leq -\frac{k_{co}}{4}\|\mathbf{Y}_o\|^2 - \frac{k_{bo}}{2}\|\tilde{W}_b\|^2 - \frac{k_{\sigma o}}{2}\|\tilde{W}_\sigma\|_F^2 + \eta_o \quad (38)$$

where  $\eta_o = \sup_{t \geq 0} \frac{k_{bo}}{2}\|\tilde{W}_b\|^2 + \frac{k_{\sigma o}}{2}\|\tilde{W}_\sigma\|_F^2 + \epsilon_1\alpha_b + \frac{\epsilon_2}{4}\|\alpha_\sigma\|^2$ . Let  $\underline{\delta} > 1 - \|\tilde{R}(0)\|_I$  and consider Lemma 2. Thereby, one obtains

$$\mathcal{L}\mathcal{U}_o \leq -\frac{\underline{\delta}k_{co}}{2}\|\tilde{R}_o\|_I - \frac{k_{bo}}{2}\|\tilde{W}_b\|^2 - \frac{k_{\sigma o}}{2}\|\tilde{W}_\sigma\|_F^2 + \eta_o \quad (39)$$

where  $\underline{\delta} = \inf_{t \geq 0} \frac{\lambda \underline{M}}{4}$ . As a result, one obtains

$$\begin{aligned} \mathcal{L}V &\leq -e_o^\top \underbrace{\begin{bmatrix} \frac{\underline{\delta}k_{co}}{2} & 0 & 0 \\ 0 & \frac{k_{bo}}{2} & 0 \\ 0 & 0 & \frac{k_{\sigma o}}{2} \end{bmatrix}}_{H_3} e_o + \eta_o \\ &\leq -\lambda(H_3)\|e_o\|^2 + \eta_o \end{aligned} \quad (40)$$

with  $e_o = [\sqrt{\|\tilde{R}_o\|_I}, \|\tilde{W}_b\|, \|\tilde{W}_\sigma\|_F]^\top$ . Since  $k_{co} > 0$ ,  $k_{bo} > 0$ , and  $k_{\sigma o} > 0$ , it becomes obvious that  $\lambda(H_3) > 0$ . Thus,  $\mathcal{L}\mathcal{U}_o < 0$  if

$$\|e_o\|^2 > \frac{\eta_o}{\lambda(H_3)}$$

Hence, one has

$$\frac{d\mathbb{E}[\mathcal{U}_o]}{dt} = \mathbb{E}[\mathcal{L}\mathcal{U}_o] \leq -\frac{\lambda(H_3)}{\lambda(H_2)}\mathbb{E}[\mathcal{U}_o] + \eta_o \quad (41)$$

Hence, it can be concluded that  $e_o$  is almost SGUUB completing the proof. ■

## V. FILTER-BASED CONTROLLER FOR ATTITUDE TRACKING

In this Section, our objective is to design control laws for the attitude tracking problem reliant on the attitude estimate and direct onboard measurements such that 1) measurement uncertainties are accounted for, 2) unknown disturbances are rejected, and 3) overall stability (interconnection between controller and estimator) is guaranteed. Define the desired attitude as  $R_d \in \mathbb{SO}(3)$  and the desired angular velocity as  $\Omega_d \in \mathbb{R}^3$ . Let the error between the true and the desired attitude be

$$\tilde{R}_c = RR_d^\top \in \mathbb{SO}(3) \quad (42)$$

Let the error between the true and the desired angular velocity be

$$\tilde{\Omega}_c = R_d^\top(\Omega_d - \Omega) \in \mathbb{R}^3 \quad (43)$$

From (6), let  $d$  be an unknown disturbance attached to the control input and define  $\hat{d}$  as the estimate of  $d$ . Let the error between  $\hat{d}$  and  $d$  be

$$\tilde{d} = d - \hat{d} \quad (44)$$

**Assumption 1.** *The desired angular velocity is smooth, continuous, and uniformly upper-bounded by a scalar  $\gamma_\Omega < \infty$  with  $\gamma_\Omega \geq \max\{\sup_{t \geq 0} \|\Omega_d\|, \sup_{t \geq 0} \|\dot{\Omega}_d\|\}$ . Also, the unknown disturbances are uniformly upper-bounded by a scalar  $\|d\| \leq \gamma_d < \infty$ .*

The desired attitude dynamics are given by

$$\dot{R}_d = R_d[\Omega_d]_\times \quad (45)$$

From (22),  $M_r \tilde{R}_c = M_r RR_d^\top = \sum_{i=1}^N s_i \mathbf{r}_i \mathbf{r}_i^\top RR_d^\top$ . Thus, one is able to show that

$$M_r \tilde{R}_c = \sum_{i=1}^N s_i \mathbf{r}_i \mathbf{y}_i^\top R_d^\top \quad (46)$$

with  $s_i$  denoting the sensor trust level of the  $i$ th measurement.

### A. Control Law from Direct Measurements and Estimated States

Consider the following control law design:

$$\begin{cases} \mathbf{Y}_c &= \mathbf{Y}(M_r \tilde{R}_c) = \sum_{i=1}^N s_i R_d \mathbf{y}_i \times \mathbf{r}_i \\ \mathcal{T} &= J\dot{\Omega}_d - [J(\Omega_m - \hat{W}_b)]_\times \Omega_d - \hat{d} - w_c \\ w_c &= k_{c1} R_d^\top \mathbf{Y}_c + k_{c2}(\Omega_m - \hat{W}_b - \Omega_d) \\ \hat{d} &= \frac{k_d}{k_{c1}}(\Omega_m - \hat{W}_b - \Omega_d) - \gamma_d k_d \hat{d} \end{cases} \quad (47)$$

where  $k_{c1}$ ,  $k_{c2}$ ,  $k_d$ , and  $\gamma_d$  are positive constants,  $\hat{W}_b$  is the estimate of  $W_b$ ,  $\hat{d}$  is the estimate of  $d$ , and  $w_c$  is an innovation term.

**Theorem 2.** *Consider the dynamics in (11) with the rotational torque  $\mathcal{T}$  being defined as in (47). Let the control law in (47) be coupled with the filter design in (31) such that the attitude and the unknown weighted bias are estimated using the filter design in (31). Then, all the closed-loop error signals of the filter-based controller ( $\|\tilde{R}_o\|_I$ ,  $\tilde{W}_b$ ,  $\tilde{W}_\sigma$ ,  $\|\tilde{R}_c\|_I$ ,  $\tilde{\Omega}_c$ ,  $\tilde{d}$ ) are SGUUB.*

*Proof:* Recall the attitude error in (42), the attitude dynamics in (6), and the desired attitude dynamics in (45). Accordingly, one finds the attitude error dynamics as below:

$$\begin{aligned} \dot{\tilde{R}}_c &= R[\Omega]_\times R_d^\top - R[\Omega_d]_\times R_d^\top \\ &= \tilde{R}_c[R_d(\Omega - \Omega_d)]_\times = \tilde{R}_c[\tilde{\Omega}_c]_\times \end{aligned} \quad (48)$$

with  $\tilde{\Omega}_c = R_d(\Omega - \Omega_d)$ . Defining  $\|M_r \tilde{R}_c\|_I = \frac{1}{4}\text{Tr}\{M_r(\mathbf{I}_3 - \tilde{R}_c)\}$  and recalling (11) and (12), one finds

$$\frac{d}{dt}\|M_r \tilde{R}_c\|_I = \frac{1}{2}\mathbf{Y}(M_r \tilde{R}_c)^\top \tilde{\Omega}_c \quad (49)$$

In view of (43), (47), and (48), one obtains

$$\begin{aligned} \frac{d}{dt} J R_d^\top \tilde{\Omega}_c &= [J\Omega]_\times R_d^\top \tilde{\Omega}_c + [\Omega_d]_\times J \tilde{W}_b - w_c + \tilde{d} \\ &\quad - [Jn]_\times \Omega_d \end{aligned} \quad (50)$$

It becomes apparent that

$$\begin{aligned} \frac{d}{dt} \tilde{\Omega}_c &= -R_d(J^{-1}[J\Omega]_\times + k_{c2}J^{-1} + [\Omega]_\times) R_d^\top \tilde{\Omega}_c \\ &\quad + R_d^\top J^{-1}(k_{c2}\mathbf{I}_3 - [\Omega_d]_\times J) \tilde{W}_b \\ &\quad - k_{c1} R_d J^{-1} R_d^\top \Upsilon(M_r \tilde{R}_c) + R_d J^{-1} \tilde{d} \end{aligned} \quad (51)$$

In addition, one finds

$$\Upsilon(\dot{\tilde{R}}_c) = \frac{1}{2}(\text{Tr}\{\tilde{R}_c\}\mathbf{I}_3 - \tilde{R}_c)^\top \tilde{\Omega}_c = \frac{1}{2}\Psi(\tilde{R}_c)\tilde{\Omega}_c \quad (52)$$

Note that in view of Lemma 2

$$\lambda_{\overline{M}_r}^2 \|\tilde{R}_c\|_I \leq \|\Upsilon(M_r \tilde{R}_c)\|^2 \leq \bar{\lambda}_{\overline{M}_r}^2 \|\tilde{R}_c\|_I$$

with  $\overline{M}_r = \text{Tr}\{M_r\}\mathbf{I}_3 - M_r$ . Define  $\delta_{c1}$  as a positive constant. Therefore, from (51) and (52), one has

$$\begin{aligned} &\frac{1}{\delta_{c1}} \frac{d}{dt} \Upsilon(\tilde{R}_c)^\top \tilde{\Omega}_c \\ &= -\frac{1}{\delta_{c1}} \left( \frac{d}{dt} \Upsilon(\tilde{R}_c)^\top \right) \tilde{\Omega}_c - \frac{1}{\delta_{c1}} \Upsilon(\tilde{R}_c)^\top \left( \frac{d}{dt} R_d \tilde{\Omega}_c \right) \\ &\leq \left( \frac{c_{c3}}{\delta_{c1}} \|\tilde{\Omega}_c\| + \frac{c_{c3}}{\delta_{c1}} \|\tilde{W}_b\| + \frac{c_{c3}}{\delta_{c1}} \|\tilde{d}\| \right) \sqrt{\|\tilde{R}_c\|_I} \\ &\quad - \frac{k_{c1} c_{c2}}{\delta_{c1}} \|\tilde{R}_c\|_I \end{aligned} \quad (53)$$

where  $\gamma_\Omega \geq \max\{\sup_{t \geq 0} \|\Omega_d\|\}$ ,  $c_{c1} = \max\{\sup_{t \geq 0} \|J^{-1}\|_F, \sup_{t \geq 0} \|J^{-1}[J\Omega]_\times + k_{c2}J^{-1} + [\Omega]_\times\|_F, \sup_{t \geq 0} \|J^{-1}(k_{c2}\mathbf{I}_3 - [\Omega_d]_\times J)\|_F\}$ ,  $c_{c2} = \min\{\frac{\lambda_{\overline{M}_r}}{\lambda_J}\}$ , and  $c_{c3} = \max\{\frac{1}{2} + c_{c1}\bar{\lambda}_{\overline{M}_r}, k_{c2} + \bar{\lambda}_J \gamma_\Omega\}$ . Define the following Lyapunov function candidate  $\mathcal{U}_c = \mathcal{U}_c(\|M_r \tilde{R}_c\|_I, R_d \tilde{\Omega}_c, \tilde{d})$ :

$$\begin{aligned} \mathcal{U}_c &= 2\|M_r \tilde{R}_c\|_I + \frac{1}{2k_{c1}} \tilde{\Omega}_c^\top R_d^\top J R_d \tilde{\Omega}_c + \frac{1}{\delta_{c1}} \Upsilon(\tilde{R}_c)^\top \tilde{\Omega}_c \\ &\quad + \frac{1}{2k_d} \tilde{d}^\top \tilde{d} \end{aligned} \quad (54)$$

where  $\mathcal{U}_c : \mathbb{S}\mathbb{O}(3) \times \mathbb{R}^3 \times \mathbb{R}^3 \rightarrow \mathbb{R}_+$ . Considering Lemma 2, one obtains

$$\begin{aligned} &e_c^\top \underbrace{\begin{bmatrix} \frac{\lambda_{\overline{M}_r}}{2\delta_{c1}} & -\frac{1}{2\delta_{c1}} & 0 \\ -\frac{1}{2\delta_{c1}} & \frac{1}{2k_{c1}} & 0 \\ 0 & 0 & \frac{1}{2k_d} \end{bmatrix}}_{H_4} e_c \\ &\leq \mathcal{U}_c \leq e_c^\top \underbrace{\begin{bmatrix} \frac{\bar{\lambda}_{\overline{M}_r}}{2\delta_{c1}} & \frac{1}{2\delta_{c1}} & 0 \\ \frac{1}{2\delta_{c1}} & \frac{1}{2k_{c1}} & 0 \\ 0 & 0 & \frac{1}{2k_d} \end{bmatrix}}_{H_5} e_c \end{aligned}$$

where  $e_c = \left[ \sqrt{\|\tilde{R}_c\|_I}, \|\tilde{\Omega}_c\|, \|\tilde{d}\| \right]^\top$ . It becomes apparent that for  $\frac{\lambda_{\overline{M}_r}}{2\delta_{c1}} > \sqrt{\frac{k_{c1}}{2\delta_{c1}^2}}$  and  $\frac{\bar{\lambda}_{\overline{M}_r}}{2\delta_{c1}} > \sqrt{\frac{k_{c1}}{2\delta_{c1}^2}}$ , one finds that  $\underline{\lambda}(H_4), \bar{\lambda}(H_5) > 0$  and, in turn  $\mathcal{U}_c > 0$  for all  $e_c \in \mathbb{R}^3 \setminus \{0\}$ .

Let us select  $\frac{\lambda_{\overline{M}_r}}{2\delta_{c1}} > \sqrt{\frac{k_{c1}}{2\delta_{c1}^2}}$ . Hence, from (49) and (50), one finds

$$\begin{aligned} \dot{\mathcal{U}}_c &= \Upsilon(M_r \tilde{R}_c)^\top \tilde{\Omega}_c - \frac{1}{k_d} \tilde{d}^\top \dot{\tilde{d}} + \frac{1}{\delta_{c1}} \frac{d}{dt} \Upsilon(\tilde{R}_c)^\top \tilde{\Omega}_c \\ &\quad + \frac{1}{k_{c1}} \tilde{\Omega}_c^\top R_d ([J\Omega]_\times R_d^\top \tilde{\Omega}_c + [\Omega_d]_\times J \tilde{W}_b - w_c \\ &\quad \quad \quad + \tilde{d} - [Jn]_\times \Omega_d) \end{aligned} \quad (55)$$

where  $\mathcal{L}\mathcal{U}_c = \dot{\mathcal{U}}_c$ . From (47), one obtains

$$\begin{aligned} \mathcal{L}\mathcal{U}_c &\leq -\frac{k_{c1} c_{c2}}{\delta_{c1}} \|\tilde{R}_c\|_I - \frac{2k_{c2} - 1}{2k_{c1}} \|\tilde{\Omega}_c\|^2 - \frac{1}{2} \|\tilde{d}\|^2 \\ &\quad + \left( \frac{c_{c3}}{\delta_{c1}} \|\tilde{\Omega}_c\| + \frac{c_{c3}}{\delta_{c1}} \|\tilde{d}\| \right) \sqrt{\|\tilde{R}_c\|_I} + \frac{1}{k_{c1}} \|\tilde{\Omega}_c\| \|\tilde{d}\| \\ &\quad + \left( \frac{c_{c3}}{\delta_{c1}} \sqrt{\|\tilde{R}_c\|_I} + \frac{c_1}{k_{c1}} \|\tilde{\Omega}_c\| \right) \|\tilde{W}_b\| \\ &\quad + \frac{1}{k_{c1}} \|k_{c2}n + [Jn]_\times \Omega_d\| + \frac{1}{2} \|\tilde{d}\|^2 \end{aligned} \quad (56)$$

Let us define  $\eta_c = \frac{1}{k_{c1}} \sup_{t \geq 0} \|k_{c2}n + [Jn]_\times \Omega_d\| + \frac{1}{2} \|\tilde{d}\|^2$ . Thus, the expression in (57) becomes as follows:

$$\begin{aligned} \mathcal{L}\mathcal{U}_c &\leq -e_c^\top \underbrace{\begin{bmatrix} \frac{k_{c1} c_{c2}}{\delta_{c1}} & -\frac{c_{c3}}{2\delta_{c1}} & -\frac{c_{c3}}{2\delta_{c1}} \\ -\frac{c_{c3}}{2\delta_{c1}} & \frac{2k_{c2}-1}{2k_{c1}} & \frac{1}{2k_{c1}} \\ -\frac{c_{c3}}{2\delta_{c1}} & \frac{1}{2k_{c1}} & \frac{1}{2} \end{bmatrix}}_{H_6} e_c \\ &\quad + \frac{c_{c3}}{\delta_{c1}} \|\tilde{W}_b\| \sqrt{\|\tilde{R}_c\|_I} + \frac{c_1}{k_{c1}} \|\tilde{\Omega}_c\| \|\tilde{W}_b\| + \eta_c \end{aligned} \quad (57)$$

One is able to show that  $\underline{\lambda}(H_6) > 0$  for  $\delta_{c1} > \frac{c_{c3}^2(k_{c1} + 2k_{c2} - 3)}{2k_{c1} c_{c2}(2k_{c2} - 3)}$ . Consider selecting  $\delta_{c1}$  such that  $\underline{\lambda}(H_6) > 0$ , and let  $\underline{\lambda}_{H_6} = \underline{\lambda}(H_6)$ . One has

$$\begin{aligned} \mathcal{L}\mathcal{U}_c &\leq -\underline{\lambda}_{H_6} \|e_c\|^2 + \left( \frac{c_{c3}}{\delta_{c1}} \sqrt{\|\tilde{R}_c\|_I} + \frac{c_1}{k_{c1}} \|\tilde{\Omega}_c\| \right) \|\tilde{W}_b\| \\ &\quad + \eta_c \end{aligned} \quad (58)$$

From (33) and (54), define the following Lyapunov function candidate:

$$\mathcal{U}_T = \mathcal{U}_o + \mathcal{U}_c \quad (59)$$

From (40) and (58), one obtains

$$\begin{aligned} \mathcal{L}\mathcal{U}_T &\leq -\underline{\lambda}_{H_3} \|e_o\|^2 - \underline{\lambda}_{H_6} \|e_c\|^2 + \frac{c_{c3}}{\delta_{c1}} \|\tilde{W}_b\| \sqrt{\|\tilde{R}_c\|_I} \\ &\quad + \frac{c_1}{k_{c1}} \|\tilde{\Omega}_c\| \|\tilde{W}_b\| + \eta_o + \eta_c \end{aligned} \quad (60)$$

Let  $c_c = \max\{\frac{c_{c3}}{\delta_{c1}}, \frac{c_1}{k_{c1}}\}$  and  $\eta_T = \eta_o + \eta_c$ . Thus, one shows

$$\mathcal{L}\mathcal{U}_T \leq -e_T^\top \underbrace{\begin{bmatrix} \underline{\lambda}_{H_3} & c_c \\ c_c & \underline{\lambda}_{H_6} \end{bmatrix}}_{H_T} e_T + \eta_T \quad (61)$$

where  $e_T = [\|e_o\|, \|e_c\|]^\top$ . The expression in (60) implies that  $\underline{\lambda}_{H_T} = \underline{\lambda}(H_T) > 0$  for  $\underline{\lambda}_{H_3} > \frac{c_c^2}{\underline{\lambda}_{H_6}}$ . Let us select  $\underline{\lambda}_{H_3} > \frac{c_c^2}{\underline{\lambda}_{H_6}}$ . Therefore,  $\mathcal{L}\mathcal{U}_T < 0$  if

$$\|e_T\|^2 > \frac{\eta_T}{\underline{\lambda}(H_T)}$$

Thus

$$\frac{d\mathbb{E}[\mathcal{U}_T]}{dt} = \mathbb{E}[\mathcal{L}\mathcal{U}_T] \leq -\frac{\underline{\lambda}(H_T)}{\lambda_x} \mathbb{E}[\mathcal{U}_T] + \eta_T \quad (62)$$

---

**Algorithm 1** Stochastic filter-based controller algorithm
 

---

**Initialization:**

- 1: Set  $\hat{R}[0] = \hat{R}_0 \in \mathbb{SO}(3)$ ,  $\hat{W}_b[0] = \hat{W}_{b|0} = \mathbf{0}_{3 \times 1}$ ,  $\hat{W}_\sigma[0] = \hat{W}_{\sigma|0} = \mathbf{0}_{q \times q}$ ,  $\hat{d}[0] = \hat{d}_0 = \mathbf{0}_{3 \times 1}$ ,  $s_i \geq 0$  for all  $i \geq 2$ , select  $\Gamma_\sigma, k_{ob}, k_{o\sigma}, k_{c1}, k_{c2}, k_d, \gamma_b, \gamma_d > 0$ ,  $K_\Upsilon = \text{rand}(q, 3) \in \mathbb{R}^{q \times 3}$ ,  $\Gamma_b \in \mathbb{R}^{q \times 3}$  where  $\underline{\lambda}(\Gamma_b^\top \Gamma_b) > 0$ , and set  $k = 0$ .

**while**

- 2: 
$$\begin{cases} \mathbf{r}_i &= \frac{\mathbf{r}_i}{\|\mathbf{r}_i\|}, \quad \mathbf{y}_i = \frac{\mathbf{y}_i}{\|\mathbf{y}_i\|}, \quad i = 1, 2, \dots, N \\ \hat{\mathbf{y}}_i &= \hat{R}_{k-1}^\top \mathbf{r}_i \\ \Upsilon &= \Upsilon(M_y \tilde{R}_o) = \sum_{i=1}^N \frac{s_i}{2} \hat{\mathbf{y}}_i \times \mathbf{y}_i \\ \|M_y \tilde{R}_o\|_I &= \frac{1}{4} \text{Tr}\{\sum_{i=1}^N s_i \mathbf{y}_i (\mathbf{y}_i - \hat{\mathbf{y}}_i)^\top\} \end{cases}$$
- 3: 
$$\begin{cases} \Psi_1 = (\|M_y \tilde{R}_o\|_I + 1) \exp(\|M_y \tilde{R}_o\|_I) \\ \Psi_2 = (\|M_y \tilde{R}_o\|_I + 2) \exp(\|M_y \tilde{R}_o\|_I) \end{cases}$$
- 4:  $\varphi(\Upsilon) = \tanh(K_\Upsilon \Upsilon)$  /\* hyperbolic tangent activation function \*/
- 5: 
$$\begin{cases} \hat{W}_{b|k} = \hat{W}_{b|k-1} + \Delta t \gamma_b (\Psi_1 \Gamma_b \varphi(\Upsilon) - k_{ob} \hat{W}_{b|k-1}) \\ \hat{W}_{\sigma|k} = \hat{W}_{\sigma|k-1} \\ \quad + \Delta t \Gamma_\sigma (\frac{\Psi_2}{4} \varphi(\Upsilon) \varphi(\Upsilon)^\top - k_{o\sigma} \hat{W}_{\sigma|k-1}) \end{cases}$$
- 6:  $C = \left( \Gamma_b^\top \mathbf{I}_3 + \frac{\Psi_2}{4 \Psi_1} (\Gamma_b^\top \Gamma_b) \right)^{-1} \Gamma_b^\top \hat{W}_{\sigma|k} \varphi(\Upsilon)$  /\* angle-axis parameterization \*/
- 7: 
$$\begin{cases} \eta &= (\Omega_{m|k} - \hat{W}_{b|k} - C) \Delta t \\ \beta &= \|\eta\|, \quad u = \eta / \|\eta\| \\ \mathcal{R}_{exp} &= \mathbf{I}_3 + \sin(\beta) [u]_\times + (1 - \cos(\beta)) [u]_\times^2 \end{cases}$$
- 8:  $\hat{R}_k = \hat{R}_{k-1} \mathcal{R}_{exp}$
- 8: 
$$\begin{cases} \Upsilon_c = \Upsilon(M_r \tilde{R}_c) = \sum_{i=1}^N s_i R_d \hat{\mathbf{y}}_i \times \mathbf{r}_i \\ w_c = k_{c1} R_d^\top \Upsilon_c + k_{c2} (\Omega_{m|k} - \Omega_{d|k} - \hat{W}_{b|k}) \\ \hat{d}_k &= \hat{d}_{k-1} \\ \quad + \Delta t \left( \frac{k_d}{k_{c1}} (\Omega_{d|k} - \Omega_{m|k} + \hat{W}_{b|k}) - \gamma_d k_d \hat{d}_{k-1} \right) \\ \mathcal{T} &= J \hat{\Omega}_{d|k} - [J(\Omega_{m|k} - \hat{W}_{b|k})]_\times \Omega_{d|k} - \hat{d}_k - w_c \end{cases}$$
- 9:  $k + 1 \rightarrow k$

**end while**

with  $\lambda_x = \max\{\bar{\lambda}(H_2), \bar{\lambda}(H_5)\}$ . Hence, one concludes that  $e_T$  is almost SGUUB completing the proof. ■

## VI. SUMMARY OF IMPLEMENTATION

The detailed implementation steps of the discrete NN-based nonlinear stochastic filter-based controller for the attitude tracking problem are presented in Algorithm 1. Note that  $\Delta t$  describes a small sampling time.

## VII. NUMERICAL RESULTS

This section demonstrates the effectiveness of the proposed real-time NN stochastic filter-based controller on  $SO(3)$  at a low sampling rate ( $\Delta t = 0.01$  sec). The discrete filter detailed in Algorithm 1 is validated considering large initialization error, high level of uncertainties, and unknown disturbances. Let the initial desired attitude be set as  $R_d[0] = R_{d|0} = \mathbf{I}_3 \in$

$\mathbb{SO}(3)$  and the desired angular velocity rate be

$$\hat{\Omega}_d = 0.1 \begin{bmatrix} 1 \sin(0.15t + \frac{\pi}{4}) \\ 0.5 \sin(0.1t + \frac{\pi}{3}) \\ 0.8 \cos(0.12t + \frac{\pi}{2}) \end{bmatrix}$$

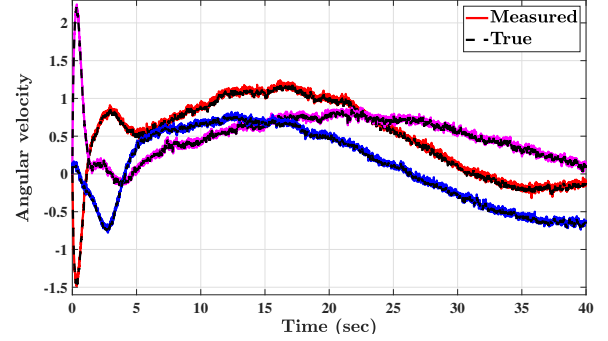


Fig. 2. Sample of angular velocity (0 to 40 seconds): Black center-line (True) vs colored solid-line (measured)

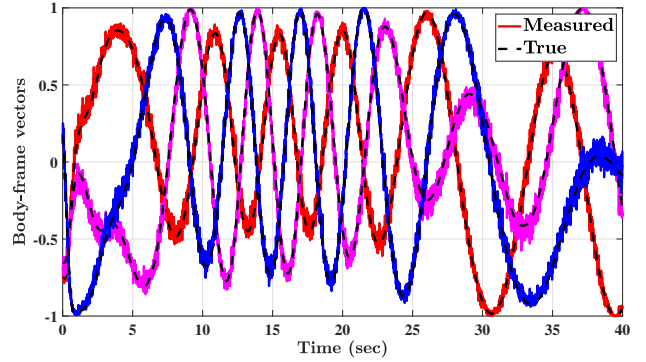


Fig. 3. Sample of vector measurements ( $y_1$ ): Black center-line (True) vs colored solid-line (measured)

Let us select the design parameters arbitrary as follows:  $k_{ob} = 1$ ,  $k_{o\sigma} = 1$ ,  $\gamma_b = 1$ ,  $\Gamma_b = 2\mathbf{I}_3$ ,  $\Gamma_\sigma = 2\mathbf{I}_3$ ,  $k_{c1} = 10$ ,  $k_{c2} = 2$ ,  $k_d = 10$ , and  $\gamma = 0.01$ . Number of neurons associated with bias and noise are selected to be both equal to three. Let the initial estimates of NN weights, disturbances, and attitude be set to  $\hat{W}_{b|0} = \hat{W}_b[0] = \mathbf{0}_{3 \times 1}$  and  $\hat{W}_{\sigma|0} = \hat{W}_\sigma[0] = \mathbf{0}_{3 \times 3}$ ,  $\hat{d}_0 = \hat{d}[0] = \mathbf{0}_{3 \times 1}$ , and  $\hat{R}(0) = \hat{R}_0 = \mathbf{I}_3 \in \mathbb{SO}(3)$ , respectively. To validate the robustness of the proposed approach against high level of uncertainties contributed by the low-cost inertial measurement unit, consider the measured angular velocity to be corrupted with unknown weighted bias  $W_b = 0.03[1, 0.5, 0.7]^\top$  (rad/sec) and normally distributed random noise  $n = \mathcal{N}(0, 0.05)$  (rad/sec) (zero mean and standard deviation of 0.05), see (9). Consider the following two observations in  $\{\mathcal{L}\}$ :  $r_1 = \frac{1}{\sqrt{3}}[1, 1, -1]^\top$  and  $r_2 = [0, 0, 1]^\top$ . Consider  $\{\mathcal{B}\}$  measurements to be corrupted by unknown bias  $b_1 = 0.05[0.2, 0.1, -0.8]^\top$  and  $b_2 = 0.05[0.5, -0.6, 0.4]^\top$  as well as normally distributed random noise  $n_1 = n_2 = \mathcal{N}(0, 0.05)$ , visit (7). Let the unknown disturbance be  $d = 0.1[1, 3, 2]^\top$  and the rigid-body's inertia matrix be  $J = \text{diag}(0.016, 0.015, 0.03)$ . To test the



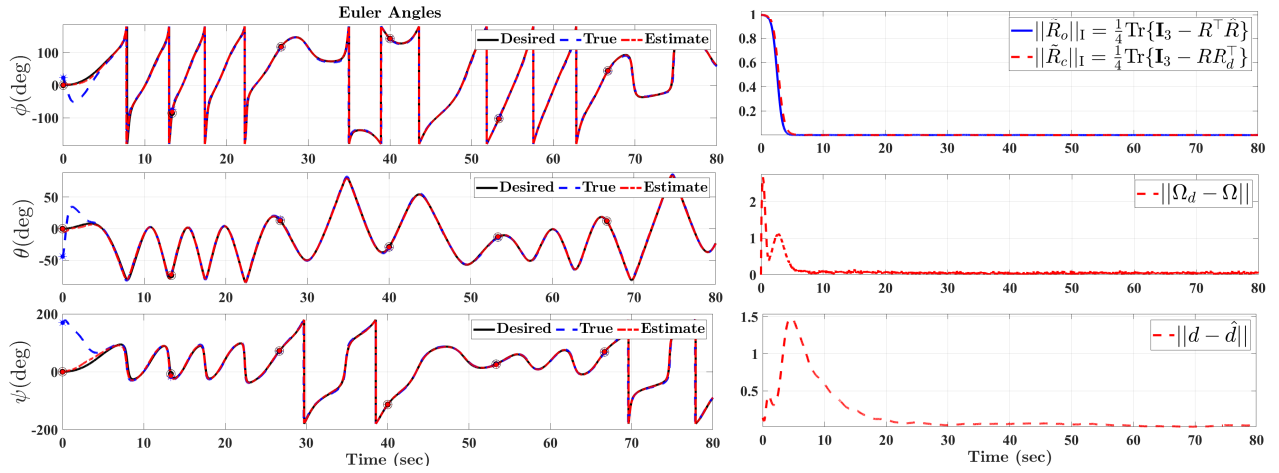


Fig. 4. Right portion demonstrates the evolution trajectories of Euler angles (desired marked as a black solid-line, true plotted as a blue dashed-line, and estimated depicted as a red center-line). Left portion illustrates the error convergence of attitude (estimation error marked as a blue solid-line and control error plotted as a red dashed-line), angular velocity (red dashed-line), and disturbance (red dashed-line) using 3 neurons.

algorithm in presence of a very large initialization error in attitude estimation and control, let the initial value of the true attitude  $R$  be

$$R[0] = \begin{bmatrix} -0.7060 & 0.0956 & 0.7018 \\ 0.1274 & -0.9576 & 0.2585 \\ 0.6967 & 0.2719 & 0.6638 \end{bmatrix} \in \mathbb{SO}(3)$$

and the initial value of the true angular velocity be  $\Omega(0) = [0.2, 0.3, 0.3]^T$  (rad/sec). Hence, one finds  $\|\tilde{R}_o(0)\|_I = \frac{1}{4}\text{Tr}\{\mathbf{I}_3 - R_0^T \hat{R}_0\} \approx 0.999$  and  $\|\tilde{R}_c(0)\|_I = \frac{1}{4}\text{Tr}\{\mathbf{I}_3 - R_0 R_{d0}^T\} \approx 0.999$  very close to the unstable equilibrium  $+1$ . Let us select hyperbolic tangent activation function  $\varphi(\alpha) = \frac{\exp(\alpha) - \exp(-\alpha)}{\exp(\alpha) + \exp(-\alpha)} \forall \alpha \in \mathbb{R}$  (see Algorithm 1, step 4).

Fig. 2 contrasts the angular velocity measurements corrupted by high level of bias and noise with the true values. Likewise, Fig. 3 presents high level of uncertainties corrupting body-frame measurements versus the true data ( $\mathbf{y}_1$ ). The left portion of Fig. 4 depicts the output performance of the true Euler angles (roll ( $\phi$ ), pitch ( $\theta$ ), yaw ( $\psi$ )), the estimated angles ( $\hat{\phi}$ ,  $\hat{\theta}$ , and  $\hat{\psi}$ ), and the desired angles ( $\phi_d$ ,  $\theta_d$ ,  $\psi_d$ ). Fig. 4 shows rapid and accurate tracking performance of the presented approach. The right portion of Fig. 4 reveals the robustness of the proposed filter-based controller in terms of error convergence of: attitude ( $\|\tilde{R}_o\|_I = \frac{1}{4}\text{Tr}\{\mathbf{I}_3 - R^T \hat{R}\}$ ) and  $\|\tilde{R}_c\|_I = \frac{1}{4}\text{Tr}\{\mathbf{I}_3 - R R_d^T\}$ ), angular velocity  $\|\Omega - \Omega_d\|$ , and disturbance  $\|d - \hat{d}\|$ . As illustrated in Fig 4, the initially very large error components converged very close to the origin. Fig. 5 presents boundedness of  $\hat{W}_b$  and  $\hat{W}_\sigma$  NN weights plotted with respect to the Euclidean and Frobenius norm, respectively. Finally, Fig. 6 shows the robustness of NN approximation in terms of transient response and steady-state error of normalized Euclidean attitude error. Although increasing the number of neurons results in reduced steady-state error, three neurons were sufficient to achieve impressive tracking performance. Table I presents statistical details of mean and standard deviation of the steady-state error values starting from 4 up to 50 seconds relative to neuron number.

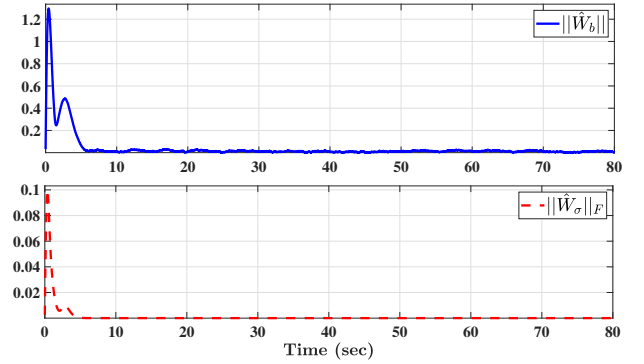


Fig. 5. Boundedness of  $\hat{W}_b$  and  $\hat{W}_\sigma$  NN weight estimates using 3 neurons.

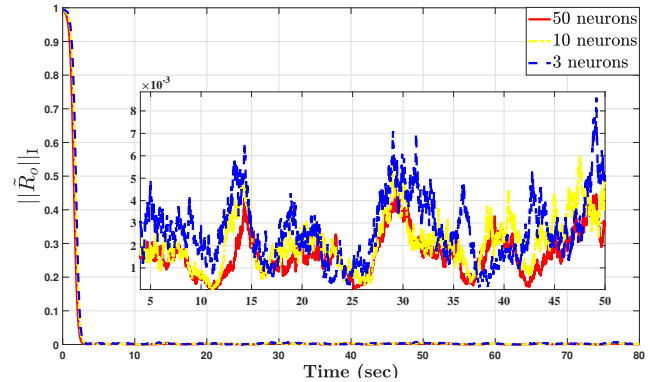


Fig. 6. Normalized Euclidean error  $\|\tilde{R}_o\|_I = \frac{1}{4}\text{Tr}\{\mathbf{I}_3 - R_k^T \hat{R}_k\}$  considering 3, 10, and 50 neurons.

TABLE I  
STEADY-STATE ERROR OF  $\|\tilde{R}_o\|_I$  VERSUS DIFFERENT NUMBER OF NEURONS.

Output results of $\ \tilde{R}_o\ _I = \frac{1}{4}\text{Tr}\{\mathbf{I}_3 - R_k^T \hat{R}_k\}$ from 4 to 50 sec			
Neurons #	3	10	50
Mean	$2.7 \times 10^{-3}$	$2.1 \times 10^{-3}$	$1.6 \times 10^{-3}$
STD	$1.5 \times 10^{-3}$	$1.2 \times 10^{-3}$	$9.2 \times 10^{-4}$

Table I shows that greater number of neurons leads to better steady-state error convergence.

### VIII. CONCLUSION

This paper presented a novel neural network (NN) stochastic filter-based controller for the attitude problem of a rigid-body rotating in three dimensional space. The proposed approach is posed on the Lie Group of the Special Orthogonal Group  $\mathbb{SO}(3)$ . Firstly, an NN-based stochastic filter design able to operate directly using measurements supplied by a local unit attached to the rigid-body has been developed. It has been demonstrated through numerical simulation that the proposed filter produces accurate estimation given measurements obtained from a low-cost inertial measurement unit. The proposed filter relies on online tuning of NN weights which are extracted using Lyapunov stability. The closed loop error signals of the proposed filter have been shown to be SGUUB. Next, a novel control law on  $\mathbb{SO}(3)$  reliant on the estimated states and uncertain measurements supplied by a low-cost onboard measurement unit has been developed. The overall stability of the filter-based controller has been confirmed and the closed loop error signals have been shown to be SGUUB. Numerical results illustrate the robustness and the fast adaptability of the proposed approach. In the future, the novel neural network (NN) stochastic filter-based controller can be reformulated to address colored noise uncertainties.

### ACKNOWLEDGMENT

#### Appendix

#### Neuro-adaptive Filter-based Controller Quaternion Representation

Let us define the three-sphere  $\mathbb{S}^3$  by

$$\mathbb{S}^3 = \{Q \in \mathbb{R}^4 \mid \|Q\| = \sqrt{q_0^2 + q^\top q} = 1\}$$

with  $Q = [q_0, q^\top]^\top \in \mathbb{S}^3$  being a unit-quaternion vector composed of two components:  $q_0 \in \mathbb{R}$  and  $q \in \mathbb{R}^3$ . The equivalent mapping  $\mathcal{R}_Q : \mathbb{S}^3 \rightarrow \mathbb{SO}(3)$  is defined by

$$\mathcal{R}_Q = (q_0^2 - \|q\|^2)\mathbf{I}_3 + 2qq^\top + 2q_0[q]_\times \in \mathbb{SO}(3) \quad (63)$$

see [40]. Let  $\hat{Q} = [\hat{q}_0, \hat{q}^\top]^\top \in \mathbb{S}^3$  denote the estimate of  $Q = [q_0, q^\top]^\top \in \mathbb{S}^3$  and  $Q_d = [q_{d0}, q_d^\top]^\top \in \mathbb{S}^3$  as the desired unit-quaternion. The quaternion representation of the NN-based nonlinear stochastic filter in (31) is given below:

$$\begin{cases} \dot{C} &= \left( \Gamma_b^\top \mathbf{I}_3 + \frac{\Psi_2}{4\Psi_1} (\Gamma_b^\top \Gamma_b)^{-1} \Gamma_b^\top \hat{W}_\sigma \right) \varphi(\mathbf{Y}_o) \\ \dot{\hat{W}}_b &= \gamma_b (\Psi_1 \Gamma_b \varphi(\mathbf{Y}_o) - k_{ob} \hat{W}_b) \\ \dot{\hat{W}}_\sigma &= \frac{\Psi_2}{4} \Gamma_\sigma \varphi(\mathbf{Y}_o) \varphi(\mathbf{Y}_o)^\top - k_{o\sigma} \Gamma_\sigma \hat{W}_\sigma \\ \dot{h} &= \Omega_m - \hat{W}_b - C \\ \mathcal{H} &= \begin{bmatrix} 0 & -h^\top \\ h & -[h]_\times \end{bmatrix} \\ \dot{\hat{Q}} &= \frac{1}{2} \mathcal{H} \hat{Q} \end{cases} \quad (64)$$

where

$$\begin{cases} \|M_y \tilde{R}_o\|_{\mathbf{I}} &= \frac{1}{4} \text{Tr} \{ \sum_{i=1}^N s_i \mathbf{Y}_i (\mathbf{y}_i - \hat{\mathbf{y}}_i)^\top \} \\ \mathbf{Y}_o &= \sum_{i=1}^N \frac{s_i}{2} \hat{\mathbf{y}}_i \times \mathbf{y}_i \\ \Psi_1 &= (\|M_y \tilde{R}_o\|_{\mathbf{I}} + 1) \exp(\|M_y \tilde{R}_o\|_{\mathbf{I}}) \\ \Psi_2 &= (\|M_y \tilde{R}_o\|_{\mathbf{I}} + 2) \exp(\|M_y \tilde{R}_o\|_{\mathbf{I}}) \end{cases} \quad (65)$$

The equivalent quaternion representation of the control law in (47) is given as follows:

$$\begin{cases} \mathbf{Y}_c &= \sum_{i=1}^N s_i \mathcal{R}_d \mathbf{Y}_i \times \mathbf{r}_i \\ \mathcal{T} &= J \hat{\Omega}_d - [J(\Omega_m - \hat{W}_b)]_\times \Omega_d - \hat{d} - w_c \\ w_c &= k_{c1} \mathcal{R}_d^\top \mathbf{Y}_c + k_{c2} (\Omega_m - \hat{W}_b - \Omega_d) \\ \hat{d} &= \frac{k_d}{k_{c1}} (\Omega_m - \hat{W}_b - \Omega_d) - \gamma_d k_d \hat{d} \end{cases} \quad (66)$$

where  $\mathcal{R}_d = (q_{d0}^2 - \|q_d\|^2)\mathbf{I}_3 + 2q_d q_d^\top + 2q_{d0}[q_d]_\times \in \mathbb{SO}(3)$ .

### REFERENCES

- [1] D. E. Zlotnik and J. R. Forbes, "Nonlinear estimator design on the special orthogonal group using vector measurements directly," *IEEE Transactions on Automatic Control*, vol. 62, no. 1, pp. 149–160, 2017.
- [2] H. A. Hashim, "Exponentially stable observer-based controller for VTOL-UAVs without velocity measurements," *International Journal of Control*, no. just-accepted, pp. 1–15, 2022.
- [3] Q. Hu, B. Jiang, and Y. Zhang, "Observer-based output feedback attitude stabilization for spacecraft with finite-time convergence," *IEEE Transactions on Control Systems Technology*, vol. 27, no. 2, pp. 781–789, 2019.
- [4] H. A. Hashim, "Systematic convergence of nonlinear stochastic estimators on the special orthogonal group  $\mathbb{SO}(3)$ ," *International Journal of Robust and Nonlinear Control*, vol. 30, no. 10, pp. 3848–3870, 2020.
- [5] R. Chai, A. Tsourdos, A. Savvaris, S. Chai, Y. Xia, and C. P. Chen, "Six-dof spacecraft optimal trajectory planning and real-time attitude control: a deep neural network-based approach," *IEEE transactions on neural networks and learning systems*, vol. 31, no. 11, pp. 5005–5013, 2020.
- [6] T. Lee, "Robust adaptive attitude tracking on  $\mathbb{SO}(3)$  with an application to a quadrotor uav," *IEEE Transactions on Control Systems Technology*, vol. 21, no. 5, pp. 1924–1930, 2012.
- [7] Y. Kuo, K. Kumar, K. Behdinan, and Z. Fawaz, "Open-loop optimal attitude control of miniature spacecraft using mems actuators," *IEEE Transactions on Aerospace and Electronic Systems*, vol. 44, no. 4, pp. 1381–1390, 2008.
- [8] M. D. Pham, K. S. Low, S. T. Goh, and S. Chen, "Gain-scheduled extended kalman filter for nanosatellite attitude determination system," *IEEE Transactions on Aerospace and Electronic Systems*, vol. 51, no. 2, pp. 1017–1028, 2015.
- [9] M. D. Shuster and S. D. Oh, "Three-axis attitude determination from vector observations," *Journal of Guidance, Control, and Dynamics*, vol. 4, pp. 70–77, 1981.
- [10] F. L. Markley, "Attitude determination using vector observations and the singular value decomposition," *Journal of the Astronautical Sciences*, vol. 36, no. 3, pp. 245–258, 1988.
- [11] D. Choukroun, I. Y. Bar-Itzhack, and Y. Oshman, "Novel quaternion kalman filter," *IEEE Transactions on Aerospace and Electronic Systems*, vol. 42, no. 1, pp. 174–190, 2006.
- [12] F. L. Markley, "Attitude error representations for kalman filtering," *Journal of guidance, control, and dynamics*, vol. 26, no. 2, pp. 311–317, 2003.
- [13] J. L. Crassidis and F. L. Markley, "Unscented filtering for spacecraft attitude estimation," *Journal of guidance, control, and dynamics*, vol. 26, no. 4, pp. 536–542, 2003.
- [14] H. A. Hashim, L. J. Brown, and K. McIsaac, "Nonlinear stochastic attitude filters on the special orthogonal group 3: Ito and stratonovich," *IEEE Transactions on Systems, Man, and Cybernetics: Systems*, vol. 49, no. 9, pp. 1853–1865, 2019.
- [15] K. S. Phogat and D. E. Chang, "Invariant extended kalman filter on matrix lie groups," *Automatica*, vol. 114, p. 108812, 2020.
- [16] M. D. Shuster, "A survey of attitude representations," *Navigation*, vol. 8, no. 9, pp. 439–517, 1993.

- [17] R. Mahony, T. Hamel, and J.-M. Pfimlin, "Nonlinear complementary filters on the special orthogonal group," *IEEE Transactions on Automatic Control*, vol. 53, no. 5, pp. 1203–1218, 2008.
- [18] Z. Zhu, Y. Xia, and M. Fu, "Adaptive sliding mode control for attitude stabilization with actuator saturation," *IEEE Transactions on Industrial Electronics*, vol. 58, no. 10, pp. 4898–4907, 2011.
- [19] A.-M. Zou, K. D. Kumar, and Z.-G. Hou, "Quaternion-based adaptive output feedback attitude control of spacecraft using chebyshev neural networks," *IEEE transactions on neural networks*, vol. 21, no. 9, pp. 1457–1471, 2010.
- [20] B. Tian, L. Yin, and H. Wang, "Finite-time reentry attitude control based on adaptive multivariable disturbance compensation," *IEEE Transactions on Industrial Electronics*, vol. 62, no. 9, pp. 5889–5898, 2015.
- [21] D. E. Zlotnik and J. R. Forbes, "Rotation-matrix-based attitude control without angular velocity measurements," in *2014 American control conference*. IEEE, 2014, pp. 4931–4936.
- [22] B. Xiao, Q. Hu, Y. Zhang, and X. Huo, "Fault-tolerant tracking control of spacecraft with attitude-only measurement under actuator failures," *Journal of Guidance, Control, and Dynamics*, vol. 37, no. 3, pp. 838–849, 2014.
- [23] F. Caccavale and L. Villani, "Output feedback control for attitude tracking," *Systems & Control Letters*, vol. 38, no. 2, pp. 91–98, 1999.
- [24] S. Salcudean, "A globally convergent angular velocity observer for rigid body motion," *IEEE transactions on Automatic Control*, vol. 36, no. 12, pp. 1493–1497, 1991.
- [25] C. G. Mayhew, R. G. Sanfelice, and A. R. Teel, "Quaternion-based hybrid control for robust global attitude tracking," *IEEE Transactions on Automatic control*, vol. 56, no. 11, pp. 2555–2566, 2011.
- [26] Z. Liu, J. Liu, and L. Wang, "Disturbance observer based attitude control for flexible spacecraft with input magnitude and rate constraints," *Aerospace Science and Technology*, vol. 72, pp. 486–492, 2018.
- [27] H. A. Hashim, M. Abouheaf, and K. G. Vamvoudakis, "Neural-adaptive stochastic attitude filter on SO(3)," *IEEE Control Systems Letters*, vol. 6, pp. 1549–1554, 2022.
- [28] Y. Zheng, J. Ma, and L. Wang, "Consensus of hybrid multi-agent systems," *IEEE transactions on neural networks and learning systems*, vol. 29, no. 4, pp. 1359–1365, 2018.
- [29] D. Chen and Y. Zhang, "Robust zeroing neural-dynamics and its time-varying disturbances suppression model applied to mobile robot manipulators," *IEEE transactions on neural networks and learning systems*, vol. 29, no. 9, pp. 4385–4397, 2018.
- [30] Y. Li, B. Niu, G. Zong, J. Zhao, and X. Zhao, "Command filter-based adaptive neural finite-time control for stochastic nonlinear systems with time-varying full-state constraints and asymmetric input saturation," *International Journal of Systems Science*, vol. 53, no. 1, pp. 199–221, 2022.
- [31] Y. Li, K. Li, and S. Tong, "Adaptive neural network finite-time control for multi-input and multi-output nonlinear systems with positive powers of odd rational numbers," *IEEE transactions on neural networks and learning systems*, vol. 31, no. 7, pp. 2532–2543, 2019.
- [32] H. F. Grip, T. I. Fossen, T. A. Johansen, and A. Saberi, "Attitude estimation using biased gyro and vector measurements with time-varying reference vectors," *IEEE Transactions on automatic control*, vol. 57, no. 5, pp. 1332–1338, 2011.
- [33] H. A. Hashim, M. Abouheaf, and M. A. Abido, "Geometric stochastic filter with guaranteed performance for autonomous navigation based on IMU and feature sensor fusion," *Control Engineering Practice*, vol. PP, no. PP, pp. 1–11, 2021.
- [34] R. Khasminskii, *Stochastic stability of differential equations*. Rockville, MD: S & N International, 1980.
- [35] K. Ito and K. M. Rao, *Lectures on stochastic processes*. Tata institute of fundamental research, 1984, vol. 24.
- [36] H.-B. Ji and H.-S. Xi, "Adaptive output-feedback tracking of stochastic nonlinear systems," *IEEE Transactions on Automatic Control*, vol. 51, no. 2, pp. 355–360, 2006.
- [37] H. Deng, M. Krstic, and R. J. Williams, "Stabilization of stochastic nonlinear systems driven by noise of unknown covariance," *IEEE Transactions on Automatic Control*, vol. 46, no. 8, pp. 1237–1253, 2001.
- [38] X. Zhao, P. Shi, X. Zheng, and J. Zhang, "Intelligent tracking control for a class of uncertain high-order nonlinear systems," *IEEE transactions on neural networks and learning systems*, vol. 27, no. 9, pp. 1976–1982, 2015.
- [39] S. M. Siniscalchi and V. M. Salerno, "Adaptation to new microphones using artificial neural networks with trainable activation functions," *IEEE transactions on neural networks and learning systems*, vol. 28, no. 8, pp. 1959–1965, 2016.
- [40] H. A. Hashim, "Special orthogonal group SO(3), euler angles, angle-axis, rodriguez vector and unit-quaternion: Overview, mapping and challenges," *arXiv preprint arXiv:1909.06669*, 2019.



**Hashim A. Hashim** (Senior Member, IEEE) is an Assistant Professor with the Department of Mechanical and Aerospace Engineering, Carleton University, Ottawa, Ontario, Canada. From 2019 to 2021, he was an Assistant Professor with the Department of Engineering and Applied Science, Thompson Rivers University, Kamloops, British Columbia, Canada.

He received the B.Sc. degree in Mechatronics, Department of Mechanical Engineering from Helwan University, Cairo, Egypt, the M.Sc. in Systems and Control Engineering, Department of Systems Engineering from King Fahd University of Petroleum & Minerals, Dhahran, Saudi Arabia, and the Ph.D. in Robotics and Control, Department of Electrical and Computer Engineering at Western University, Ontario, Canada.

His current research interests include vision-based aided navigation and control, localization and mapping, stochastic and deterministic estimation, sensor fusion, and distributed control of multi-agent systems.



**Kyriakos G. Vamvoudakis** (Senior Member, IEEE) was born in Athens, Greece. He received the diploma degree in electronic and computer engineering from the Technical University of Crete, Crete, Greece, in 2006, and the M.Sc. and Ph.D. degrees in electrical engineering from The University of Texas, Arlington, TX, USA, in 2008 and 2011, respectively.

From 2012 to 2016, he was a Research Scientist with the Center for Control, Dynamical Systems and Computation, University of California at Santa Barbara, Santa Barbara, CA, USA. He was an Assistant Professor with the Kevin T. Crofton Department of Aerospace and Ocean Engineering, Virginia Tech, Blacksburg, VA, USA, until 2018. Dr. Vamvoudakis currently serves as an Assistant Professor with The Daniel Guggenheim School of Aerospace Engineering, Georgia Tech, Atlanta, GA, USA. His research interests include reinforcement learning, game theory, cyber-physical security, and safe autonomy.

Dr. Vamvoudakis is a recipient of the 2019 ARO YIP Award, the 2018 NSF CAREER Award, the 2021 GT Chapter Sigma Xi Young Faculty Award, and of several international awards including the 2016 International Neural Network Society Young Investigator (INNS) Award.